

From Prompts to Printable Models: Support-Effective 3D Generation via Offset Direct Preference Optimization

Chenming Wu*, Xiaofan Li*, Chengkai Dai†

Abstract—The transition from digital 3D models to physical objects via 3D printing often requires support structures to prevent overhanging features from collapsing during the fabrication process. While current slicing technologies offer advanced support strategies, they focus on post-processing optimizations rather than addressing the underlying need for support-efficient design during the model generation phase. This paper introduces SEG (*Support-Effective Generation*), a novel framework that integrates Direct Preference Optimization with an Offset (ODPO) into the 3D generation pipeline to directly optimize models for minimal support material usage. By incorporating support structure simulation into the training process, SEG encourages the generation of geometries that inherently require fewer supports, thus reducing material waste and production time. We demonstrate SEG’s effectiveness through extensive experiments on two benchmark datasets, Thingi10k-Val and GPT-3DP-Val, showing that SEG significantly outperforms baseline models such as TRELIS, DPO, and DRO in terms of support volume reduction and printability. Qualitative results further reveal that SEG maintains high fidelity to input prompts while minimizing the need for support structures. Our findings highlight the potential of SEG to transform 3D printing by directly optimizing models during the generative process, paving the way for more sustainable and efficient digital fabrication practices.

I. INTRODUCTION

Imagine a world where the digital creations that spark our imagination can seamlessly transition from the screen to our hands. In recent years, the rapid advancements in 3D generation models, particularly those utilizing diffusion techniques, have opened the doors to unprecedented possibilities in digital fabrication. These models, capable of producing intricate and diverse geometries from simple textual descriptions, are not just tools for artists and designers; they represent a paradigm shift in how we conceive and interact with objects in our environment.

As we increasingly rely on digital assets, the potential to transform these virtual creations into tangible forms becomes a vital step in enhancing our daily lives. Personalized fabrication through 3D printing allows us to materialize ideas that were once confined to screens, creating a bridge between the digital and physical worlds. Whether it’s custom-designed home decor, medical implants tailored to individual patients, or educational tools that bring concepts to life, the implications of this technology are profound. The ability to produce unique, on-demand objects can radically change how we think about consumption, creativity, and accessibility.

However, this exciting potential is accompanied by significant challenges. One of the most pressing issues in

translating 3D-generated models into printable objects is the necessity of support structures. Existing text-to-3D models ignore printability constraints, while slicers handle support after geometry is fixed. These supports are crucial for maintaining the integrity of overhanging features during the printing process. Yet, they often lead to material waste and extended production times, and they can compromise the surface quality of the final product [1], [2]. Traditional geometric optimization approaches have proven effective by either deforming the 3D model in the post-processing phase [3] or decomposing the model into a sequence of subparts for multi-axis fabrication [4], [5]. Unfortunately, many existing 3D generation models fail to account for these practical constraints during their training, resulting in geometries that, while visually stunning, may not be feasible for real-world fabrication.

Recognizing these challenges, we set out to create a solution that not only enhances the capabilities of 3D generation but also aligns them with the practical realities of 3D printing. We introduce SEG, a novel framework that employs Direct Preference Optimization with an Offset (ODPO) [6] to refine generative models specifically for support-efficient object creation. By integrating simulation-based feedback on support structure volume into the alignment objective, SEG encourages the generation of geometries that require fewer supports while maintaining the fidelity and aesthetic appeal of the designs. Our contributions can be summarized as follows:

- We introduce SEG, the first framework that refines 3D generative models for support-efficient design.
- We employ ODPO to incorporate support-effective constraints into the generation process, which effectively handles skewed reward distributions.
- Our experiments validate the effectiveness of SEG in a text-to-3D context, demonstrating consistent support-volume reduction and comparable geometric fidelity.

II. RELATED WORK

A. Support-oriented Modeling and Optimization

Support-oriented modeling and optimization methods are designed to create 3D shapes that can be fabricated with minimal or no additional support structures by embedding printability constraints directly within the modeling process. This approach addresses a fundamental challenge in 3D printing—especially in Fused Filament Fabrication (FFF)—where steep overhangs and unsupported features typically require supplementary supports to prevent collapse

*Contributed equally. †Corresponding authors.

during printing. The use of these supports is undesirable, as it leads to increased material consumption, extended printing times, and often leaves behind rough or blemished surfaces after support removal [7].

Prior research in support-aware modeling primarily focused on post-processing strategies that modify a completed model to reduce the need for supports or to enhance its structural stability. For example, build-orientation optimization algorithms evaluate various possible orientations of a given part, seeking to minimize the area of unsupported faces or to reduce the average angle of overhangs [8], [9]. Once an orientation is selected, explicit support-generation methods design and position support structures—ranging from tree-like branches [10] to locally adaptive struts that are strategically placed according to geometric needs [11], [12]. These algorithms aim to uphold problematic features while balancing the trade-offs between print duration and material efficiency. Another class of techniques, partitioning-based methods, decompose complex models into smaller, more manageable sub-parts that can each be printed with fewer supports, subsequently reassembling them via geometric joints or adhesives [13].

By contrast, more recent approaches integrate support constraints directly into the modeling phase, rather than treating support generation as a secondary step. For instance, topology optimization under overhang constraints incorporates additional penalties—such as those based on feature angles or surface curvature—into classical density-based solvers, thereby discouraging the formation of unprintable regions during the design process [14], [15]. Other methods operate directly on the mesh geometry, applying curvature-driven smoothing to eliminate sharp overhangs, or enforcing manufacturability criteria such as minimum wall thickness and maximum unsupported span [3].

While these methods have proven effective for individual models, their reliance on case-by-case optimization or heuristic adjustment poses significant challenges for scalability.

B. Text-to-3D Generation

Text-to-3D model generation, or text-to-3D modeling, translates natural-language prompts into three-dimensional shapes by weaving semantic alignment directly into the geometry creation process. Just as support-aware modeling bakes physical manufacturing constraints into design, text-to-3D pipelines embed language-driven objectives at generation time.

One of the primary paradigms is per-prompt optimization, which sculpts a dedicated 3D representation for each input by iteratively applying Score Distillation Sampling from a frozen text-to-image diffusion model through a differentiable renderer. DreamFusion [16] pioneered this approach by refining a neural radiance field (NeRF) to match the input text. Magic3D [17] accelerates this process with a two-stage, coarse-to-fine latent diffusion pipeline and hash-grid volumetric representation, while DreamGaussian [18] abandons NeRFs in favor of 3D Gaussian splatting to achieve synthesis

in minutes. ProlificDreamer [19] then incorporates variational score distillation to jointly improve visual fidelity and sample diversity, and TextMesh [20] adds a signed-distance-function backbone to produce watertight, mesh-extractable outputs directly from text prompts. However, these methods incur heavy per-prompt computation—often on the order of minutes to hours per input—limiting interactive editing and rapid iteration.

Another key paradigm is amortized feed-forward generation, which eliminates per-prompt loops by training a single network to map text embeddings directly to 3D outputs in a single forward pass. ATT3D [21] distills multi-view diffusion guidance into a prompt-conditioned NeRF generator for one-shot synthesis. LATTE3D [22] scales this approach with greater capacity and diversity. GET3D [23] trains a GAN to produce textured triangle meshes from latent codes. Shap-E [24] synthesizes continuous implicit fields on demand; Point-E [25] hierarchically upsamples low-resolution point clouds to full geometry. and TRELIS [26] introduces Structured 3D Latent representations and rectified flow transformers to generate versatile, high-quality 3D assets across multiple output formats (e.g., NeRF, Gaussian, mesh). These approaches achieve real-time throughput but focus exclusively on visual and semantic objectives.

While per-prompt methods excel in fidelity and amortized methods in speed, neither paradigm embeds physical or fabrication-aware objectives into the generation process. To address this gap, recent work integrates physical simulation or fabrication constraints directly into 3D generative pipelines to ensure stability. For example, Atlas3D [27] augments Score Distillation Sampling with a differentiable stability loss under gravity, contact, and friction to produce text-conditioned models that stand unaided in both simulation and real-world tests. Recently, Direct Simulation Optimization (DSO) utilizes non-differentiable simulator scores to label generated shapes and refines a diffusion-based 3D generator through Direct Preference Optimization for physical soundness [28]. While stability or soundness can be assessed by the absolute simulated value, our focus on support efficiency aims to minimize the support structures needed for 3D models during physical fabrication. This approach encourages the generation of geometries that inherently require minimal support when produced.

III. PROPOSED METHOD

Our proposed method is built upon a pretrained diffusion-based 3D generative model $\pi_\theta(x|y)$, where y is a text prompt and x is the latent code for a mesh \mathcal{M} . Our method is to align π_θ with the preference of support-effective printing so that the generated mesh \mathcal{M} requires minimal support structure volume $V(\mathcal{M}_{sup})$ when fabricated using common 3D printing processes.

For clarity, we begin by detailing the fundamentals of support structures in 3D printing, explaining the computational methods employed. Next, we describe how to efficiently simulate the support structure of a generated sample (mesh) using ray tracing and geometric approximation. We

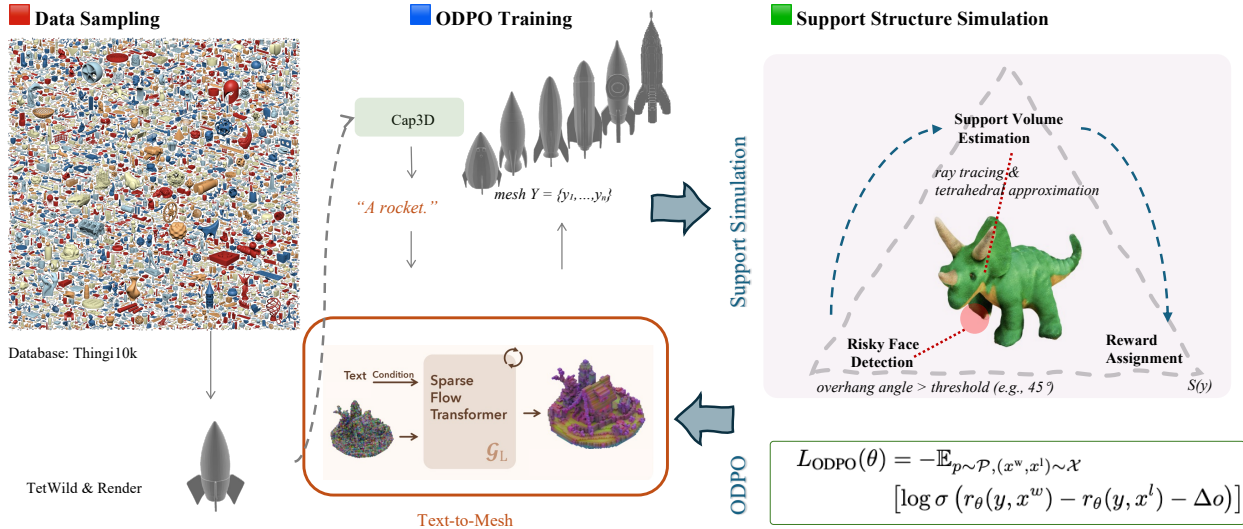


Fig. 1: **Overview of the proposed SEG pipeline.** The process begins with data sampling from the Thingi10k database, where multi-view images are generated and captioned using Cap3D. The Text-to-Mesh transformation utilizes a sparse flow transformer G_L for model generation. Subsequently, the ODPO training phase incorporates support structure simulation, which includes estimating support volume, identifying risky faces, and assigning rewards based on overlap detection. This integrated approach facilitates the effective generation of 3D models with optimized support requirements.

then discuss the preference alignment method we proposed, followed by an overview of the preference data construction pipeline we developed for training our network. An overview of our proposed SEG can be referred to Fig. 1.

A. Support Structure Simulation

In 3D printing, a model \mathcal{M} is deposited layer by layer along a specified printing direction \mathbf{d} . Following the definitions of the maximal self-support angle α_{max} and self-supported regions as described in [3], [29], [4], we categorize the faces of \mathcal{M} based on their printability. Specifically, for any face with normal vector \mathbf{n} , it is considered *safe* if it satisfies the following condition:

$$\mathbf{n} \cdot \mathbf{d} + \sin(\alpha_{max}) \geq 0, \quad (1)$$

indicating that the face can be printed without additional support. Faces that do not meet this criterion are labeled as *risky*, as they are prone to requiring support structures during fabrication. To address this, segmentation-based methods have been developed to modify the geometry of \mathcal{M} , aiming to eliminate or reduce the presence of risky faces and thus improve overall printability. Although the risky angle depends on the printing device chosen, we use a widely-used value of $\alpha_{max} = 45^\circ$ in the following context.

An illustrative example of risky face identification and support generation is presented in Fig. 2. The volumes of \mathcal{M} and \mathcal{M}_{sup} can be efficiently computed as $V(\mathcal{M})$ and $V(\mathcal{M}_{sup})$, respectively. However, since the volumes of different meshes can vary significantly, making fair comparisons of support effectiveness is challenging. To address this issue, we propose a simple yet effective metric called the normalized support volume (NSV), which normalizes the

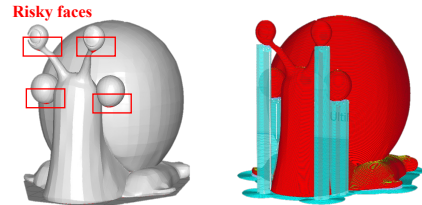


Fig. 2: An example of the generated mesh featuring risky faces (left) alongside the sliced visualization, highlighting areas that require additional support in blue (right).

support volume by the volume of the mesh. Specifically, NSV is defined as:

$$\text{NSV}(\mathcal{M}, \mathcal{M}_{sup}) = \frac{V(\mathcal{M}_{sup})}{V(\mathcal{M})} \quad (2)$$

To efficiently evaluate NSV of support structures, we utilize Axis-Aligned Bounding Boxes (AABB) for rapid computation of the volume from risky faces to the print bed. This is achieved using the Embree [30], which facilitates fast AABB calculations to determine the spatial relationship between the model's faces and the print surface. For each risky face, we compute its AABB and determine the intersection points with the print surface. If the risky face intersects with the print surface, we consider the volume above it as potential support volume. Given the small area of the face, we approximate the volume using three tetrahedra, which allows for a more accurate representation of the geometry. The volume V of each tetrahedron can be computed using

the formula:

$$V = \frac{1}{6} \begin{vmatrix} x_1 & y_1 & z_1 & 1 \\ x_2 & y_2 & z_2 & 1 \\ x_3 & y_3 & z_3 & 1 \\ x_4 & y_4 & z_4 & 1 \end{vmatrix}$$

where (x_i, y_i, z_i) are the coordinates of the tetrahedron’s vertices. The total volume V_{total} from the three tetrahedra can then be expressed as:

$$V_{\text{total}} = V_1 + V_2 + V_3 \quad (3)$$

By summing the volumes of the constructed tetrahedra, the simulation effectively estimates the total support volume extending from each risky face to either the print bed or its terminating height. This formulation allows the model to account for the structural stability required during fabrication. It is worth noting that our approach is agnostic to the specific support simulation method. In essence, the support simulation S proceeds by (1) identifying risky faces, (2) locating their intersection points with either the print bed or the mesh surface, and (3) accumulating the volumes of all resulting tetrahedra.

B. Formulating Alignment with ODPO

The primary objective of this work is to guide the generative process such that models requiring minimal support structures are preferentially favored. In other words, we aim to align the generation objective with the reduction of support volume: the fewer support structures a model necessitates, the higher the score or reward it should receive during evaluation. Given a set of generated 3D models’ latents $\mathcal{X} = \{x_0, \dots, x_n\}$ and the corresponding text prompts $\mathcal{P} = \{y_0, \dots, y_N\}$, the support structure required to print it along its upright direction can be simulated as $S(x_0)$, which can be either represented by the volume of the supports or the area of the risky faces. However, no matter which representation we choose, it is an absolute metric used for geometric computing. A straightforward method following [28] is to formulate the alignment similar to Diffusion-DPO [31]. That is, we first enumerate the above simulated samples to a list of pairwise win-loss tuples $\mathcal{X}^{\text{pair}}$, any pair of them is a tuple of (x^w, x^l) , where w denotes win and l denotes lose. Following [31], the training loss is defined as follows.

$$\mathcal{L}_{\text{DPO}} = -\mathbb{E}_{y \sim \mathcal{P}, (x^w, x^l) \sim \mathcal{X}} [\text{logsigmoid}(r_\theta(x^w) - r_\theta(x^l))] \quad (4)$$

where r is the reward model.

This DPO paradigm can be trained using the samples generated by our simulator. However, upon analyzing the data distribution in the dataset, we find that training the model using the difference in NSV results in uniformly obtained samples, most of which are clustered closely together. In other words, our alignment task poses challenges due to the reward values not being constrained to the range of 0 to 1; they can either be significantly large or very small, often close to each other. This lack of diversity in the

training samples does not provide sufficient information for the network to converge effectively.

We devise a solution to this problem by prompting the diffusion model to increase the likelihood of preferred responses compared to dispreferred ones through a penalization mechanism. This mechanism can be viewed as an ‘offset’ based on the difference in their respective reward values. To effectively optimize our model, we employ ODPO [6], which involves introducing an offset Δo that accounts for the differences in the reward values between preferred and dispreferred samples. Specifically, we define Δo based on the extent of preference indicated by the NSV values $r(y, x^w)$ and $r(y, x^l)$ for the preferred response x^w and dispreferred response x^l , respectively.

$$\Delta o = \alpha f (r'(y, x^w) - r'(y, x^l)) \quad (5)$$

where α is a hyperparameter that controls the extent to which the offset should be enforced, and f is a monotonically increasing function, and we propose to use $f = \log$ in our method. Here we use the NSV metric to compute r' . The loss function for ODPO can then be formulated as:

$$L_{\text{ODPO}}(\theta) = -\mathbb{E}_{y \sim \mathcal{P}, (x^w, x^l) \sim \mathcal{X}} [\log \sigma (r_\theta(y, x^w) - r_\theta(y, x^l) - \Delta o)] \quad (6)$$

where $r_\theta(x, y)$ represents the estimated reward for the response given the prompt. By applying this loss function, we ensure that the model increases the likelihood of the preferred response x^w over the dispreferred response x^l by an offset that reflects their relative quality.

This approach enhances our model’s ability to align with human preferences more accurately, particularly in scenarios where the reward values vary widely. By prioritizing larger differences in rewards while still learning from smaller distinctions, ODPO significantly improves the fine-tuning process of our DPO model.

C. Preference Construction

Our work specifically addresses the application of 3D printing (3DP), utilizing the Thingi10k dataset [32], which is widely recognized in the 3DP research community. Notably, some raw data in the [32] dataset contain non-manifold faces, leading to inconsistencies in data curation. To preprocess the dataset, we employ the method described in [33], which involves tetrahedralization to extract manifold surfaces.

For data curation in our training process, we begin by rendering multi-view images of models from the Thingi10k dataset, generating eight distinct views for each model to aid in text captioning. We employ Cap3D [34] to create high-quality and detailed captions with minimal hallucination, resulting in a total of 9,840 prompt-model pairs. Subsequently, we utilize the methodology outlined in [26] to sample ten different latent representations for each prompt. Finally, we apply the aforementioned support structure simulation approach to determine the requisite support volume and NSV for training purposes.

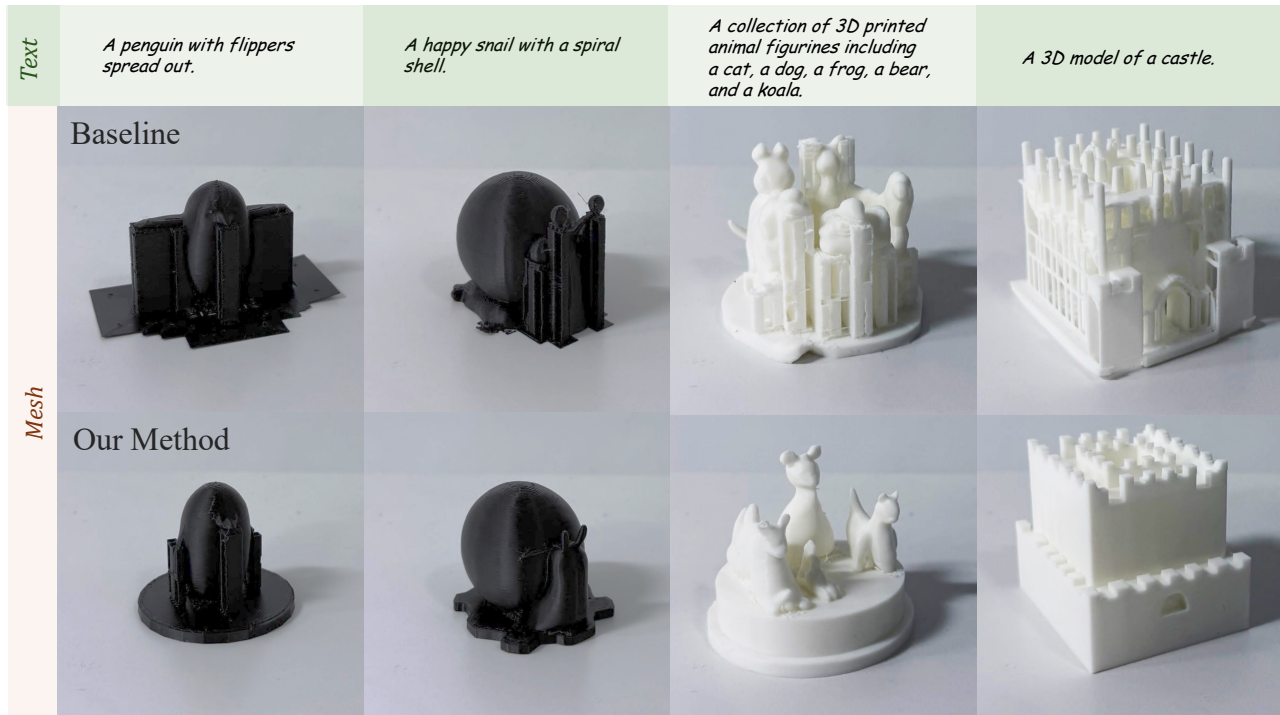


Fig. 3: We present the printed results of models generated by the baseline approach (top), which necessitate substantial support structures during the printing process to ensure printability. In contrast, the models produced by our proposed SEG framework (bottom) demonstrate a significantly more efficient requirement for support structures.

IV. RESULTS

A. Experimental Setup

We train our proposed SEG model using $8 \times$ NVIDIA A100 GPUs, each of which has 40GB VRAM, leveraging DeepSpeed [35] with ZeRO-1 offload for enhanced performance. The learning rate is configured to 5×10^{-6} , and we utilize a batch size of 96 per iteration through gradient accumulation, completing a total of 50,000 training steps with the Adam optimizer [36]. Our foundation is the state-of-the-art 3D diffusion-based generative model TRELIS (text-to-3D, XL size) [26], which serves as a robust starting point. To efficiently validate our proposed method, we use LoRA [37] training with rank of 64 and alpha of 128. For ODPO, the α is set to 1. This approach enables effective fine-tuning while preserving the model’s original capabilities.

a) Benchmark Datasets: To validate the effectiveness of our proposed method in terms of support-efficient 3D printing (3DP), we created two benchmark datasets. The first benchmark dataset, named *Thing10k-Val*, is derived from the aforementioned curated dataset, where we split the entire Thing10k [32] dataset into training and validation sets. The validation set consists of 100 prompts randomly selected from this split.

We also utilize GPT-4.1 to generate 60 prompts specifically designed for 3D generation in daily life, animation, and animal categories. These prompts were selected with a focus on scenarios likely to require support structures, ensuring that we account for cases that are too straightforward and do

not necessitate supports, such as a simple cube. This dataset is referred to as *GPT-3DP-Val* in the following context.

b) Evaluation Metrics: We utilize the NSV metric to evaluate the support structures generated by our proposed method and the baseline models, as it directly relates to the goal of support-efficient 3D generation. To extend NSV metric from a single model to the whole dataset, we define the volume-weighted NSV as the default computation method, and denote the arithmetic mean of NSV values as NSV^* . Additionally, different models may yield varying results for the same prompt, allowing us to assess the rate considering the cases of both win and tie (under a threshold of 10^{-3}) based on NSV across the entire benchmark dataset, a measure we refer to as support-efficient consistency (SEC). This metric offers an alternative means of evaluating the consistency of support structure reduction while reducing the impact of randomness.

c) Baselines: Our model is built upon a pretrained diffusion-based 3D generation framework, which provides a solid foundation for our approach. We specifically select the pretrained model, referred to as TRELIS [18]. In addition to this strong baseline, we train two more models using vanilla Direct Preference Optimization (DPO) and the Direct Reward Optimization (DRO) [28]. These comparisons are primarily aimed at assessing physical stability, enabling us to evaluate the effectiveness of our approach in enhancing the robustness and reliability of the generated 3D models.

TABLE I: Quantitative evaluation across different baselines on Thingi10k-Val.

Method	Thingi10k-Val		
	NSV↓	NSV* ↓	SEC↑
TRELLIS	0.343	1.255	N/A
DPO	0.310	1.200	0.740
DRO	5.999	18.467	0.070
Ours	0.176	0.587	0.870

TABLE II: Quantitative evaluation across different baselines on GPT-3DP-Val.

Method	GPT-3DP-Val		
	NSV↓	NSV* ↓	SEC↑
TRELLIS	0.504	1.265	N/A
DPO	0.432	1.021	0.733
DRO	6.128	19.642	0.067
Ours	0.222	0.691	0.867

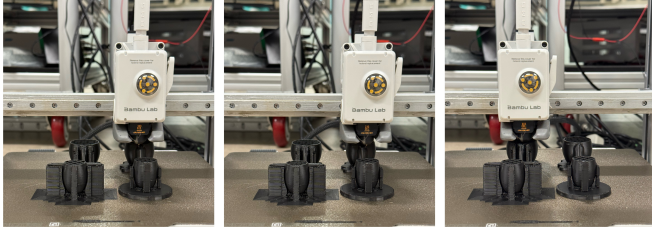


Fig. 4: 3D printing process using the Bambu Lab A1 printer for models generated by both the baseline diffusion model and our optimized approach.

B. Quantitative Results

We conducted experiments on two validation datasets. The results of these evaluations are summarized in Tab. I and Tab. II. Our findings reveal that our method consistently outperforms all other evaluated techniques across both datasets. Notably, we observed a decline in performance following training with the DRO-based approach. We attribute this deterioration to the incompatibility of directly using NSV as a reward during training, as well as the absence of a reference model, which contributed to instability throughout the training process. These outcomes not only highlight the effectiveness and robustness of our proposed approach but also emphasize its potential to significantly advance the field of 3D generation.

We present visualizations of the results generated by our method in comparison to the baseline model in Fig. 5. To enhance clarity, we have highlighted the areas deemed risky in red, indicating regions that necessitate the addition of support structures to prevent the collapse of overhanging sections during the printing process. Furthermore, we have fabricated several pairs of results using the Bambu Labs A1 3D printer, as depicted in Fig. 4. This practical demonstration, featured in Fig. 3, underscores the potential applications of our method in real-world physical printing scenarios.

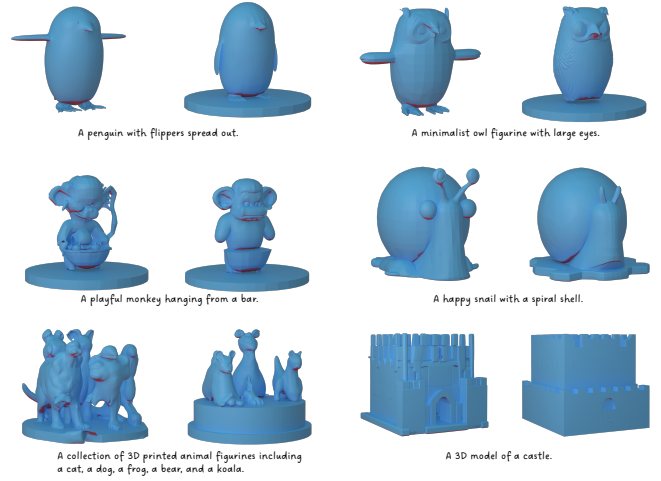


Fig. 5: More visualization results generated by TRELLIS [26] (left) and our model (right). The models are colored in blue, while the risky areas are highlighted in red.

The ability to generate 3D models that maintain structural integrity while minimizing support requirements represents a significant advancement in the field of 3D model generation.

TABLE III: Statistics of the ablation study.

	NSV↓	NSV* ↓	SEC↑
$\alpha = 2$	0.516	3.468	0.590
w/o offset	0.310	1.200	0.740
early stop	0.242	0.864	0.790
full	0.176	0.587	0.870

C. Ablation Study

We perform an ablation study to evaluate the impact of various design choices. The quantitative results of our experiments are presented in Tab. III, including a larger value of $\alpha = 2$, the absence of an offset, and an early stopping criterion at half the total iterations (*i.e.*, 25K). The results clearly demonstrate that our full model achieves the best performance across all three metrics: NSV, NSV*, and SEC. This highlights the significance of our design choices.

D. Discussions

Our approach is a preliminary effort to fine-tune a diffusion-based 3D generative model for specific applications, though some limitations remain. The reliance on the manifold assumption for simulating support structures may introduce biases, especially when dealing with double-sided meshes or floating facets. These issues are not inherent to our method and could be addressed with future geometry-assured 3D generation models. While SEG primarily targets FDM printers with a standard self-support angle, it is flexible and can be extended to other 3D printing technologies like SLA and SLS. Future work will explore optimizing upright orientation and self-support angles to enhance support efficiency across different printing methods.

V. CONCLUSION

This paper introduces the SEG framework, which uses ODPO to enhance 3D generative models for support-efficient printing. By addressing the critical issue of support structures, often overlooked during model training, SEG aims to make digital fabrication more sustainable and accessible. The primary reason SEG achieves consistent improvements is that ODPO reshapes the training signal distribution, amplifying meaningful preference differences in NSV. This prevents collapse in regions where support rewards are sparse. Future work will refine SEG and explore additional constraints for improved printability.

REFERENCES

- [1] W. Gao, Y. Zhang, D. Ramanujan, K. Ramani, Y. Chen, C. B. Williams, C. C. Wang, Y. C. Shin, S. Zhang, and P. D. Zavattieri, "The status, challenges, and future of additive manufacturing in engineering," *Computer-Aided Design*, vol. 69, pp. 65–89, 2015.
- [2] X. Zhang, X. Le, A. Pantopoulou, E. Whiting, and C. C. L. Wang, "Perceptual models of preference in 3d printing direction," *ACM Trans. Graph.*, vol. 34, no. 6, pp. 215:1–215:12, Oct. 2015.
- [3] K. Hu, S. Jin, and C. C. Wang, "Support slimming for single material based additive manufacturing," *Computer-Aided Design*, vol. 65, pp. 1–10, 2015.
- [4] C. Wu, C. Dai, G. Fang, Y.-J. Liu, and C. C. Wang, "General support-effective decomposition for multi-directional 3-d printing," *IEEE Transactions on Automation Science and Engineering*, vol. 17, no. 2, pp. 599–610, 2019.
- [5] C. Dai, C. C. Wang, C. Wu, S. Lefebvre, G. Fang, and Y.-J. Liu, "Support-free volume printing by multi-axis motion," *ACM Transactions on Graphics (TOG)*, vol. 37, no. 4, pp. 1–14, 2018.
- [6] A. Amini, T. Vieira, and R. Cotterell, "Direct preference optimization with an offset," *arXiv preprint arXiv:2402.10571*, 2024.
- [7] W. Gao, Y. Zhang, D. Ramanujan, K. Ramani, Y. Chen, C. B. Williams, C. C. Wang, Y. C. Shin, S. Zhang, and P. D. Zavattieri, "The status, challenges, and future of additive manufacturing in engineering," *Computer-Aided Design*, vol. 69, pp. 65–89, 2015.
- [8] J. Dumas and S. Lefebvre, "Efficient computation of support structures in 3d printing," in *ACM SIGGRAPH 2014 Posters*, 2014, pp. 1–1.
- [9] R. Paul and S. Anand, "Optimization of layered manufacturing process for reducing form errors with minimal support structures," *Journal of Manufacturing Systems*, vol. 36, pp. 231–243, 2015.
- [10] B. Vaissier, J.-P. Pernot, L. Chougrani, and P. Véron, "Genetic-algorithm based framework for lattice support structure optimization in additive manufacturing," *Computer-Aided Design*, vol. 110, pp. 11–23, 2019.
- [11] J. Vanek, J. A. G. Galicia, and B. Benes, "Clever support: Efficient support structure generation for digital fabrication," *Computer Graphics Forum*, vol. 33, no. 5, pp. 117–125, 2014.
- [12] T. Wang, S. Gao, L. Wang, Y. Liu, L. Liu, and T. Ju, "Supportnet: Efficient and accurate support generation for additive manufacturing," in *Computer Graphics Forum*, vol. 37, no. 7. Wiley Online Library, 2018, pp. 177–187.
- [13] L. Luo, I. Baran, S. Rusinkiewicz, and W. Matusik, "Chopper: partitioning models into 3d-printable parts," *ACM Trans. Graph.*, vol. 31, no. 6, Nov. 2012.
- [14] A. T. Gaynor and J. K. Guest, "Topology optimization considering overhang constraints: Eliminating sacrificial support material in additive manufacturing through design," *Structural and Multidisciplinary Optimization*, vol. 54, no. 5, pp. 1157–1172, 2016.
- [15] M. Langelaar, "An additive manufacturing filter for topology optimization of print-ready designs," *Structural and Multidisciplinary Optimization*, vol. 55, no. 3, pp. 871–883, 2017.
- [16] B. Poole, A. Jain, J. T. Barron, D. B. Brooks, B. D. Ziebart, and B. Mildenhall, "Dreamfusion: Text-to-3d using 2d diffusion models," *arXiv preprint arXiv:2209.14988*, 2022.
- [17] C.-H. Lin, J. Gao, L. Tang, T. Takikawa, X. Zeng, X. Huang, K. Kreis, S. Fidler, M.-Y. Liu, and T.-Y. Lin, "Magic3d: High-resolution text-to-3d content creation," in *Proceedings of the IEEE/CVF Conference on Computer Vision and Pattern Recognition (CVPR)*, June 2023, pp. 300–309.
- [18] J. Tang, J. Ren, H. Zhou, Z. Liu, and G. Zeng, "Dreamgaussian: Generative gaussian splatting for efficient 3d content creation," *arXiv preprint arXiv:2309.16653*, 2023.
- [19] Z. Wang, C. Lu, Y. Wang, F. Bao, C. Li, H. Su, and J. Zhu, "Prolificdreamer: High-fidelity and diverse text-to-3d generation with variational score distillation," in *Advances in Neural Information Processing Systems (NeurIPS)*, 2023.
- [20] C. Tsalicoglou, F. Manhardt, A. Tonioni, M. Niemeyer, and F. Tombari, "Textmesh: Generation of realistic 3d meshes from text prompts," in *2024 International Conference on 3D Vision (3DV)*, 2024, pp. 1554–1563.
- [21] J. Lorraine, K. Xie, X. Zeng, C.-H. Lin, T. Takikawa, N. Sharp, T.-Y. Lin, M.-Y. Liu, S. Fidler, and J. Lucas, "Att3d: Amortized text-to-3d object synthesis," in *2023 IEEE/CVF International Conference on Computer Vision (ICCV)*, 2023, pp. 17900–17910.
- [22] K. Xie, J. Lorraine, T. Cao, J. Gao, J. Lucas, A. Torralba, S. Fidler, and X. Zeng, "Latte3d: Large-scale amortized text-to-enhanced3d synthesis," *The 18th European Conference on Computer Vision (ECCV)*, 2024.
- [23] J. Gao, T. Shen, Z. Wang, W. Chen, K. Yin, D. Li, O. Litany, Z. Gojcic, and S. Fidler, "Get3d: A generative model of high quality 3d textured shapes learned from images," in *Advances In Neural Information Processing Systems*, 2022.
- [24] H. Jun and A. Nichol, "Shap-e: Generating conditional 3d implicit functions," 05 2023.
- [25] A. Nichol, H. Jun, P. Dhariwal, P. Mishkin, and M. Chen, "Point-e: A system for generating 3d point clouds from complex prompts," *arXiv preprint arXiv:2212.08751*, 2022.
- [26] J. Xiang, Z. Lv, S. Xu, Y. Deng, R. Wang, B. Zhang, D. Chen, X. Tong, and J. Yang, "Structured 3d latents for scalable and versatile 3d generation," *arXiv preprint arXiv:2412.01506*, 2024.
- [27] Y. Chen, T. Xie, Z. Zong, X. Li, F. Gao, Y. Yang, Y. N. Wu, and C. Jiang, "Atlas3d: Physically constrained self-supporting text-to-3d for simulation and fabrication," *arXiv preprint arXiv:2405.18515*, 2024.
- [28] R. Li, C. Zheng, C. Rupprecht, and A. Vedaldi, "Dso: Aligning 3d generators with simulation feedback for physical soundness," *arXiv preprint arXiv:2503.22677*, 2025.
- [29] C. Wu, C. Dai, G. Fang, Y.-J. Liu, and C. C. Wang, "Robofdm: A robotic system for support-free fabrication using fdm," in *2017 IEEE International Conference on Robotics and Automation (ICRA)*. IEEE, 2017, pp. 1175–1180.
- [30] I. Wald, S. Woop, C. Benthin, G. S. Johnson, and M. Ernst, "Embree: a kernel framework for efficient cpu ray tracing," *ACM Transactions on Graphics (TOG)*, vol. 33, no. 4, pp. 1–8, 2014.
- [31] B. Wallace, M. Dang, R. Rafailov, L. Zhou, A. Lou, S. Purushwalkam, S. Ermon, C. Xiong, S. Joty, and N. Naik, "Diffusion model alignment using direct preference optimization," in *Proceedings of the IEEE/CVF Conference on Computer Vision and Pattern Recognition*, 2024, pp. 8228–8238.
- [32] Q. Zhou and A. Jacobson, "Thing10k: A dataset of 10,000 3d-printing models," *arXiv preprint arXiv:1605.04797*, 2016.
- [33] Y. Hu, T. Schneider, B. Wang, D. Zorin, and D. Panozzo, "Fast tetrahedral meshing in the wild," *ACM Transactions on Graphics (TOG)*, vol. 39, no. 4, pp. 117–1, 2020.
- [34] T. Luo, C. Rockwell, H. Lee, and J. Johnson, "Scalable 3d captioning with pretrained models," *Advances in Neural Information Processing Systems*, vol. 36, pp. 75307–75337, 2023.
- [35] J. Rasley, S. Rajbhandari, O. Ruwase, and Y. He, "Deepspeed: System optimizations enable training deep learning models with over 100 billion parameters," in *Proceedings of the 26th ACM SIGKDD international conference on knowledge discovery & data mining*, 2020, pp. 3505–3506.
- [36] D. P. Kingma and J. Ba, "Adam: A method for stochastic optimization," *arXiv preprint arXiv:1412.6980*, 2014.
- [37] E. J. Hu, Y. Shen, P. Wallis, Z. Allen-Zhu, Y. Li, S. Wang, L. Wang, W. Chen, et al., "Lora: Low-rank adaptation of large language models," *ICLR*, vol. 1, no. 2, p. 3, 2022.